Journal of Drug Delivery Science and Technology 63 (2021) 102529

Contents lists available at ScienceDirect

Journal of Drug Delivery Science and Technology

journal homepage: www.elsevier.com/locate/jddst

Research paper

Multicomponent crystalline solid forms of aripiprazole produced via hot melt extrusion techniques: An exploratory study

Arun Butreddy [a], Mashan Almutairi [a,b], Neeraja Komanduri [a], Suresh Bandari [a], Feng Zhang [c], Michael A. Repka [a,d,*]

[a] Department of Pharmaceutics and Drug Delivery, School of Pharmacy, The University of Mississippi, University, MS, 38677, USA
[b] Department of Pharmaceutics, College of Pharmacy, University of Hail, Hail, 81442, Saudi Arabia
[c] College of Pharmacy, The University of Texas at Austin, Austin, TX, 78712, USA
[d] Pii Center for Pharmaceutical Technology, The University of Mississippi, University, MS, 38677, USA

ARTICLE INFO

Keywords:
Salts
Eutectics
Hot melt extrusion
Dissolution rate
Microenvironmental pH

ABSTRACT

Multicomponent crystalline solid forms (salts, cocrystals and eutectics) are a promising means of enhancing the dissolution behavior of poorly soluble drugs. The present study demonstrates the development of multicomponent solid forms of aripiprazole (ARP) prepared with succinic acid (SA) and nicotinamide (NA) as coformers using the hot melt extrusion (HME) technique. The HME-processed samples were characterized and analyzed using differential scanning calorimetry (DSC), hot stage microscopy (HSM), Fourier transform infrared (FTIR) spectroscopy, powder X-ray diffraction (PXRD) and scanning electron microscopy (SEM). The DSC and HSM analyses revealed a characteristic single melting temperature in the solid forms, which differed from the melting points of the individual components. The discernible changes in the FTIR (amide C═O stretching) and PXRD results for ARP-SA confirm the formation of new crystalline solid forms. In the case of ARP-NA, these changes were less prominent, without the appearance or disappearance of peaks, suggesting no change in the crystal lattice. The SEM images demonstrated morphological differences between the HME-processed samples and the individual parent components. The in vitro dissolution and microenvironment pH measurement studies revealed that ARP-SA showed a higher dissolution rate, which could be due to the acidic microenvironment pH imparted by the coformer. The observations of the present study demonstrate the applicability of the HME technique for the development of ARP multicomponent solid forms.

1. Introduction

Solid-state property improvements hold great potential for overcoming the low aqueous solubility and bioavailability issues of poorly soluble active pharmaceutical ingredients (APIs). Multicomponent crystalline solid forms of poorly soluble drugs, including cocrystals, salts and eutectics, have gained increasing interest in the alteration of the physicochemical properties of APIs [1,2]. The development of cocrystals or salts is the most effective strategy and is used in the pharmaceutical industry to enhance the dissolution rate [3]. Moreover, 40% of approved drug products and 90% of new chemical entities in the pipeline have limited aqueous solubility [4]. Therefore, modification of API solid-state properties by the design of multicomponent crystalline solid forms could be an effective approach for improving the solubility, dissolution rate, stability and mechanochemical properties of APIs [5,6].

A salt is defined as a solid-state crystalline material produced when proton transfer occurs between molecules containing acidic and basic moieties, which requires an ionizable group in the API [7]. On the other hand, cocrystal formation is an interaction between the drug and coformer by noncovalent interactions such as hydrogen bonding, π−π stacking, and van der Waals forces [5]. Similar to salts and cocrystals, eutectics are formed from two or more molecules, but the individual components (drug and coformer) in the eutectics retain their crystal structure [8]. A eutectic is a multicomponent crystalline material of two or more components that do not interact to form a new crystal lattice, but at certain points, depending on the temperature and molar ratio, both components become miscible with a melting temperature lower than the individual parent components. Eutectics have specific properties of each individual component, but other characteristics, such as the solubility and dissolution rate, may be different. In recent years, eutectic

* Corresponding author. Department of Pharmaceutics and Drug Delivery, School of Pharmacy, The University of Mississippi, University, MS, 38677, USA.
E-mail address: marepka@olemiss.edu (M.A. Repka).

https://doi.org/10.1016/j.jddst.2021.102529
Received 29 January 2021; Received in revised form 10 April 2021; Accepted 11 April 2021
Available online 20 April 2021
1773-2247/

mixtures have gained significant interest as a drug delivery approach owing to their potential to improve the physicochemical properties of drug molecules [9].

Several aspects that need to be considered when designing new multicomponent crystalline solid forms (salts, cocrystals and eutectics) include the nature of drug and coformer molecules, the influence of parent molecular components that are responsible for intermolecular interactions, the position of functional groups in the drug and coformer molecules, and the interaction strength [10]. The type of intermolecular interaction between the drug and coformer is based on molecular site recognition and the rearrangement of the components into different molecular networks [2]. Characterization tools such as differential scanning calorimetry (DSC), Fourier transform infrared (FTIR) spectroscopy can be used as preliminary indicators to differentiate the obtained multicomponent forms depending on the melting point and the shifts, appearance or disappearance of functional groups.

Different solvent-free and solid-state techniques for preparing cocrystals and salts include ball milling and hot melt extrusion (HME). HME is widely used to produce cocrystals and salts owing to advantages such as being single step, solvent free and readily scalable and having continuous manufacturing techniques [11,12]. The HME technique utilizes a combination of both melting and mixing of the drug and coformer molecules via the use of temperature and shear [4]. In recent years, coprocessing of an API and coformer in the presence of a polymer has been investigated as a matrix- or polymer-assisted cocrystallization technique to make extrusion possible and to improve the processability and throughput during extrusion. However, the amount of polymer required for matrix-assisted cocrystallization needs careful investigation to avoid the formation of multicomponent or ternary amorphous matrices [13,14].

In the past, the ability of aripiprazole (ARP) to form cocrystals has been investigated with coformers, namely, resorcinol, catechol, hydroquinone, pyrogallol, phloroglucinol, and orcinol, using traditional methods such as solvent evaporation and liquid-assisted grinding [15,16]. Ana Fernández Casares et al. [17] studied the salts of aripiprazole with succinic acid using three salt screening methods: an in situ salt screen, saturated solution and the cooling evaporative approach. Nonetheless, the study mainly focused on salt screening, and key solid-state analyses and pharmaceutical property assessments, such as dissolution studies of the obtained salts, were not performed.

Aripiprazole, a basic drug with a pKa of 7.4 and an aqueous solubility of 0.007 mg/mL, was selected as the model drug [18]. The coformers succinic acid (SA) and nicotinamide (NA) (Fig. 1) were chosen to assess the formation of multicomponent solid forms, such as salts, cocrystals or eutectics. The properties of the drug and coformers are listed in Table 1.

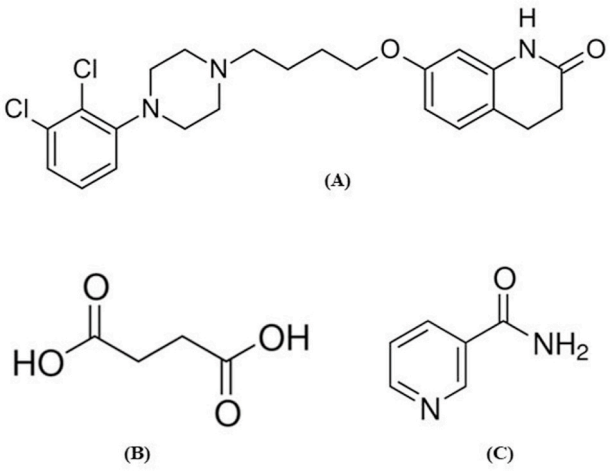

Fig. 1. Chemical structures of A) aripiprazole, B) succinic acid, and C) nicotinamide.

Table 1
Properties of the drug and coformers used in the study [1,19–21].

Material	pKa	Nature	Aqueous solubility (mg/mL)	No of hydrogen bond donors	No of hydrogen bond acceptors
ARP	7.46	Basic	0.007	1	4
SA	4.24	Acidic	71	2	4
NA	3.4	Basic	>100	1	2

Initially, the potential for salt, cocrystal or eutectic formation of ARP was evaluated by solvent evaporation (SE) as a prototype method to confirm the identity of the new multicomponent crystalline solid form. The novelty of the current investigation is the production and characterization of multicomponent crystalline solid forms of ARP using the HME technique. Furthermore, DSC, hot stage microscopy (HSM), FTIR, powder X-ray diffraction (PXRD), scanning electron microscopy (SEM), and dissolution studies were performed to confirm the formation of suitable multicomponent crystalline systems of ARP.

2. Materials and methods

2.1. Materials

ARP was obtained from Nexconn Pharmatechs Ltd. (Tseung Kwan O, Hong Kong). The coformers SA and NA were purchased from Spectrum Quality Products, Inc. (Gardena, CA, USA). All the chemicals were used as received without further purification.

2.2. Methods

2.2.1. Solvent evaporation

The multicomponent crystalline solid system of ARP with SA and NA coformers was produced by the solvent evaporation method and used as a prototype prior to HME processing. Briefly, equimolar amounts of ARP and individual coformers were dissolved in the cosolvent of dichloromethane and ethanol at a 4:1 vol ratio. The resulting solution was left for evaporation at room temperature for 72 h. The obtained powders were collected and initially characterized for the formation of a multicomponent system using DSC and FTIR.

2.2.2. HME processing

The physical mixture (PM) of ARP and its coformers (SA and NA) with 2.5% poly(ethylene oxide) (PEO) was passed through a US #30 mesh sieve and blended using a Maxiblend blender (GlobePharma, New Brunswick, New Jersey, USA) at 25 rpm for 10 min. Then, the blended PM was fed into an 11 mm corotating twin screw extruder (Process 11, Thermo Fisher Scientific, Waltham, Massachusetts, USA) at a feed rate of 0.4 g/min and screw speed of 50 rpm using a varied screw configuration of three mixing zones (high shear) and two mixing zones (low shear). ARP was extruded individually with each coformer under similar processing conditions to understand the extrusion feasibility of plain ARP with individual coformers. The extruder barrel temperature was operated at 105 °C (ARP-NA) and 125 °C (ARP-SA). During the extrusion process, the torque values were monitored throughout each run. The extrudate product obtained after the extrusion process was stored in a vacuum desiccator until further analysis.

2.2.3. DSC analysis

The thermal properties of the solid component systems were determined using a DSC instrument (Discovery DSC25, TA Instruments, Newcastle, Delaware, USA) equipped with an RCS90 refrigerator cooling system. Approximately 6–8 mg of sample was sealed in an aluminum pan and heated from 25 °C to 200 °C at a heating rate of 10 °C/min with a nitrogen purge flow rate of 50 mL/min. The empty aluminum pan was used as a reference during the measurement.

To understand the thermal events and to identify the formation of eutectics, the binary PM of ARP with the coformer (NA) was prepared at different molar ratios (1:1, 1:2, 1:3, 2:1 and 3:1) [22]. The mixtures were heated in sealed DSC pans from 25 °C to 200 °C at a heating rate of 10 °C/min. The melting onset of the endothermic peak is considered the solidus, and the peak melting temperature (endpoint) of the DSC endothermic peak is referred to as the liquidus [23,24].

2.2.4. HSM analysis

HSM observations were made using an Agilent Cary 620 IR optical microscope (Agilent, Santa Clara, CA, USA) equipped with a hot stage (T95 LinkPad and FTIR 600, Linkam, Tadworth, UK). Powder samples of the formulations were mounted on a microscope slide, which was covered with a glass coverslip and placed on the hot-stage furnace inside the sample chamber. The samples were then heated from room temperature to 200 °C at a heating rate of 10 °C/min. Changes in melting behavior as a function of temperature were recorded as images using Linkam software.

2.2.5. FTIR

FTIR spectra of ARP, the coformers and the ARP-SA and ARP-NA systems were recorded on a Cary 660 FTIR spectrometer (Agilent Technologies, Santa Clara, California, USA) to determine the intermolecular interactions. A small amount of powder sample was placed on the diamond crystal surface and pressed using the attached arm to provide uniform solid-crystal contact. The spectra were collected in the scanning range of 600–4000 cm^{-1} with a data resolution of 4 cm^{-1} and 16 scans.

2.2.6. PXRD analysis

PXRD patterns were collected on a Rigaku X-ray system (D/MAX-2500PC, Rigaku Corp., Tokyo, Japan). The diffractograms of pure ARP, the coformers, and the multicomponent solid systems were scanned over a 2θ range of 5–40° at room temperature. The diffractogram collection parameters were Cu Kα radiation (λ = 1.54184 Å), voltage of 40 kV, current of 40 mA, step width of 0.02°/s and scan speed of 2°/min.

2.2.7. SEM analysis

The morphology of the plain ARP, coformers and extruded samples was examined using a JSM-7200FLV field-emission scanning electron microscope (JOEL, Peabody, MA, USA) at an accelerated voltage of 5 kV.

Prior to imaging, the samples were scattered on the SEM stubs, adhered using double adhesive tape and then sputter coated with platinum using a fully automated Denton Desk V TSC sputter coater (Denton Vacuum, Moorestown, NJ, USA). The measurements were performed under argon atmosphere.

2.2.8. HPLC analysis

The analysis of in vitro dissolution was performed by HPLC equipped with a UV detector set at a wavelength of 248 nm. The column used was a Symmetry C18 (Waters, 100 Å, 5 μm, 4.6 mm × 150 mm), and the column temperature was maintained at 30 °C. The mobile phase consisted of 0.1% formic acid in water and acetonitrile pumped in gradient mode at a flow rate of 1.2 mL/min with an injection volume of 4 μl. The measurements were performed in triplicate.

2.2.9. Solubility and in-vitro dissolution studies

Solubility studies of ARP and eutectics or salts were performed on a shaker. Excess amounts of the ARP and its eutectics or salts were added to a vial containing 5 mL of DI water and agitated at 500 rpm, 25 °C for 48 h using a bench mark shaker (Benchmark Scientific Inc, New Jersey, USA). The samples were subsequently centrifuged for 15 min at 13000 rpm to separate the undissolved drug and the supernatant was analyzed by HPLC. For in-vitro dissolution studies, salts or eutectic extrudates equivalent to 30 mg of ARP were filled into hard gelatin capsules. Dissolution was performed in 900 mL of DI water using a USP type-II dissolution apparatus (SR8-plus, Hanson, Chatsworth, California, USA) rotating at 50 rpm and a media temperature of 37 ± 0.5 °C. One milliliter of sample was withdrawn at 10, 20, 30, 45, 60 and 120 min, filtered through a 10 μm filter (Quality Lab Accessories LLC, Pennsylvania, USA), and injected into the HPLC system to determine the amount of dissolved drug.

2.2.10. Microenvironment pH

The microenvironment pH values of ARP and the product samples of salts and eutectics were determined using the slurry method [25]. An excess amount of solid sample was placed in a 20 mL glass vial containing 10 mL DI water followed by stirring at room temperature for a period of 24 h to obtain a concentrated slurry. Subsequently, the microenvironmental pH of the samples was measured using a pH meter (Mettler Toledo). The solution pH of the pure coformers (SA and NA) was also measured under identical conditions to observe any change in the microenvironmental pH of the product samples compared to that of the pure components.

3. Results and discussion

3.1. Solvent evaporation (SE)

Prior to cocrystallization via HME, the feasibility of forming a new solid phase (cocrystals, salts or eutectics) was investigated by employing SA and NA coformers via a solvent evaporation method. DSC analysis of the product obtained after solvent evaporation showed a distinct endothermic melting peak, indicating interactions between the drug and coformer resulting in the formation of a new solid phase.

The distinct melting temperatures observed in the DSC analysis provide insights into the selection of barrel temperature in the HME process. During cocrystallization via the HME process, quality cocrystals can be produced when the processing temperature is set below the onset of the cocrystal melting temperature [26]. FTIR spectra were recorded to further confirm the formation of a new solid phase. The characteristic C═O stretching band of ARP at 1674 cm^{-1} shifted to 1685 cm^{-1} in ARP-SA and remained unchanged in the ARP-NA system. These observations suggested the transformation of ARP and the coformer into a new crystalline solid phase in the case of ARP-SA using the solvent evaporation method.

3.2. HME processing

After solvent evaporation, DSC thermograms of ARP-NA and ARP-SA were obtained, showing melting temperatures of 116 °C and 157 °C, respectively. Therefore, the barrel temperature employed during the extrusion of PM was selected to be below the melting temperature of the new solid form. In the present study, the extrusion temperatures selected for ARP-NA and ARP-SA PM were 105 °C and 125 °C, respectively, based on the salt or eutectic formation temperature in the solvent evaporation method. Since processing parameters such as screw speed (50 rpm) and feed rate (0.4 gm/min) showed no significant impact on cocrystal formation in a previous study [18], these parameters were held constant during the extrusion trials. The PM of the drug and coformer was extruded using screw configurations consisting of three mixing zones (Fig. 2A) and two mixing zones (Fig. 2B). The mixing elements in the screw configuration (Fig. 2A) were arranged at specific angles of 90° and 60° (mixing zone 1); 60° (mixing zone 2); and 30°, 60°, and 90° (mixing zone 3). These screw configurations are arranged with the intent to provide a maximum level of mixing and shear for efficient interaction or salt formation during the extrusion process. The extrusion of the PM of the drug and coformer with three mixing zones resulted in an increase in processing torque above the instrument limit (>100%). Thus, an alternative screw configuration with two mixing zones (Fig. 2B) was employed to facilitate the processing of PM components. Processing with two mixing zones did not permit the extrusion of plain PM, and

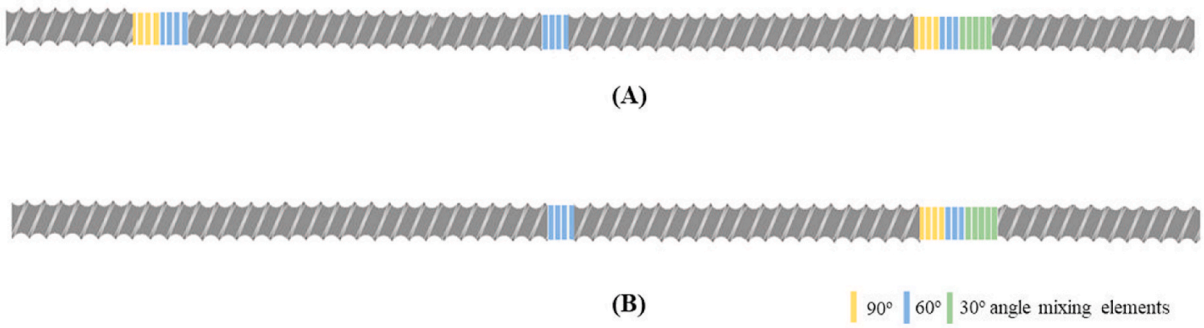

Fig. 2. Schematic representation of the different screw configurations employed in HME.

these observations are in line with previous findings [18].

The effect of the addition of 2.5% PEO (melting point (Tm) 64 °C) on the processability of an equimolar ratio of drug and coformer was investigated, and the results revealed that incorporation of the polymeric matrix significantly reduced the processing torque values (<10%) compared to those obtained with the mixture of drug and coformer. The main reason for the inclusion of PEO was to alleviate the processability issues that arise during the extrusion of plain PM components. The torque values of the extruder are well within the instrument limit at 2.5% PEO. Gajda M et al. [14] investigated the use of Kollidon VA 64 (Tg 103 °C), Soluplus (Tg 70 °C), Kollicoat IR (Tm 193 °C), and Poloxamer P407 (Tm 54 °C) HPMCAS (Tg 118 °C) as matrix polymers for cocrystallization at a level from 10 to 30 wt%. Among these polymers, Kollidon VA 64, Poloxamer P407 and Soluplus significantly reduced the torque during the extrusion process.

Sachin Korde et al. [27] investigated PEO as a pharmaceutically acceptable polymer in the mechanochemical synthesis of carbamazepine cocrystals, and the results indicated that inclusion of the polymer facilitated the processability of parent components into cocrystals. These observations suggest the applicability of a polymeric matrix in producing pharmaceutical cocrystals. However, in the present study, 2.5% PEO was selected as a matrix polymer for cocrystallization via HME, given its thermoplastic nature, melting temperature and processability at lower temperatures (below 100 °C). The processing of ARP-SA and ARP-NA PM was optimal with 2.5% PEO, three mixing zones in the screw configuration, a screw speed of 50 rpm, a feed rate of 0.4 gm/min and a temperature of 105 °C (ARP-NA) or 125 °C (ARP-SA).

3.3. DSC

Pure ARP showed a melting endotherm at 139 °C, while the coformers, namely, SA and NA, showed sharp endothermic peaks at 185 °C and 128 °C, respectively (Table 2). The melting points of HME-processed drug and coformer samples with equimolar ratios showed distinct thermal behavior with a melting endotherm lower than those of the drug and coformer for ARP-NA. It was observed that HME-produced ARP-SA with an equimolar ratio had a single melting endotherm between the pure ARP and SA melting temperatures. The absence of the melting endotherms of ARP and the coformer (SA or NA) in the ARP-SA and ARP-NA (Fig. 3A and B) systems indicated the formation of a new solid material [28].

Table 2
Melting temperature details of the drug, coformer, and multicomponent systems.

Sample details	Melting point (°C)
ARP	139.2
SA	185.2
NA	128.4
ARP-SA (SE), ARP-SA (HME)	157.7, 157.4
ARP-NA (SE), ARP-NA (HME)	115.7, 116.5

The melting point of a newly formed crystalline material is often employed to predict or differentiate eutectics or cocrystals. Traditionally, eutectics are characterized by a lower melting point than the drug and coformer. Cocrystals/salts usually exhibit intermediate or higher melting temperatures than the parent components [2]. Thermal analysis by construction of a phase diagram (Fig. 4) can be used as a complementary approach to determine whether a combination of a drug and coformer can form a cocrystal or a eutectic [22]. For eutectics, a typical binary phase diagram assumes a "V" shape, where the minimum point of the V indicates the molar ratio and melt temperature at the eutectic point. In the case of a cocrystal system, the binary thermal phase diagram appears as a "W" shape, which contains a cocrystal region between two eutectic points [29,30].

In the ARP-SA system, the first endothermic peak was observed at 137 °C, followed by a second melting peak detected at 160 °C, suggesting that the obtained solid form could be salts or cocrystals.

In the ARP-NA binary phase diagram, different molar ratios of drug and coformer exhibited only a single invariant low melting temperature at 116 °C (Fig. 3C), suggesting that ARP and NA may form a eutectic mixture as evidenced by the single endothermic peak at different molar ratios. At the other molar ratios (2:1 and 3:1) of ARP-NA PM, a second melting endotherm was observed, attributed to noneutectic or near eutectic formation due to the presence of excess ARP.

From the DSC results, we hypothesize that the ARP-SA system may result in the formation of cocrystals/salts and that the ARP-NA system may form a eutectic mixture. It has been reported in the literature that cocrystals can be formed from eutectic melts. One such system includes indomethacin-nicotinamide; in these systems, thermal analysis of the PM showed a single distinctive endothermic peak [31]. This could be due to the overlap of thermal effects, in which PM melting was observed close to the cocrystal melting temperature [32]. In some cases, the binary phase diagram is underutilized for some systems due to the complex variety of thermal transitions and difficulties observed in the interpretation of the phases involved. Hence, the application of DSC in the differentiation of cocrystals and eutectics is limited, particularly for cocrystals where two components may form eutectic mixtures. A physical mixture containing a drug and coformers may resemble a eutectic mixture during heating in DSC. It was hypothesized that a system can form eutectic cocrystals when heated in DSC beyond its eutectic temperature [22]. The close melting temperatures of ARP and NA led to the overlapping thermal effects in the physical mixtures due to the dissolution of one component in the melt of the other. Such overlapping thermal events can be seen when analyzing physical mixtures in which the melting temperatures of cocrystal components differ from each other by less than 50 °C [32]. Similar observations were reported for itraconazole-succinic acid cocrystals, where the physical mixture showed a melting endotherm at 151 °C, which is different from the melting temperatures of itraconazole (169 °C) and succinic acid (191 °C) [33]. In the ARP-NA system, the potential of cocrystal formation cannot be excluded due to the single endothermic peak in the PM, and these

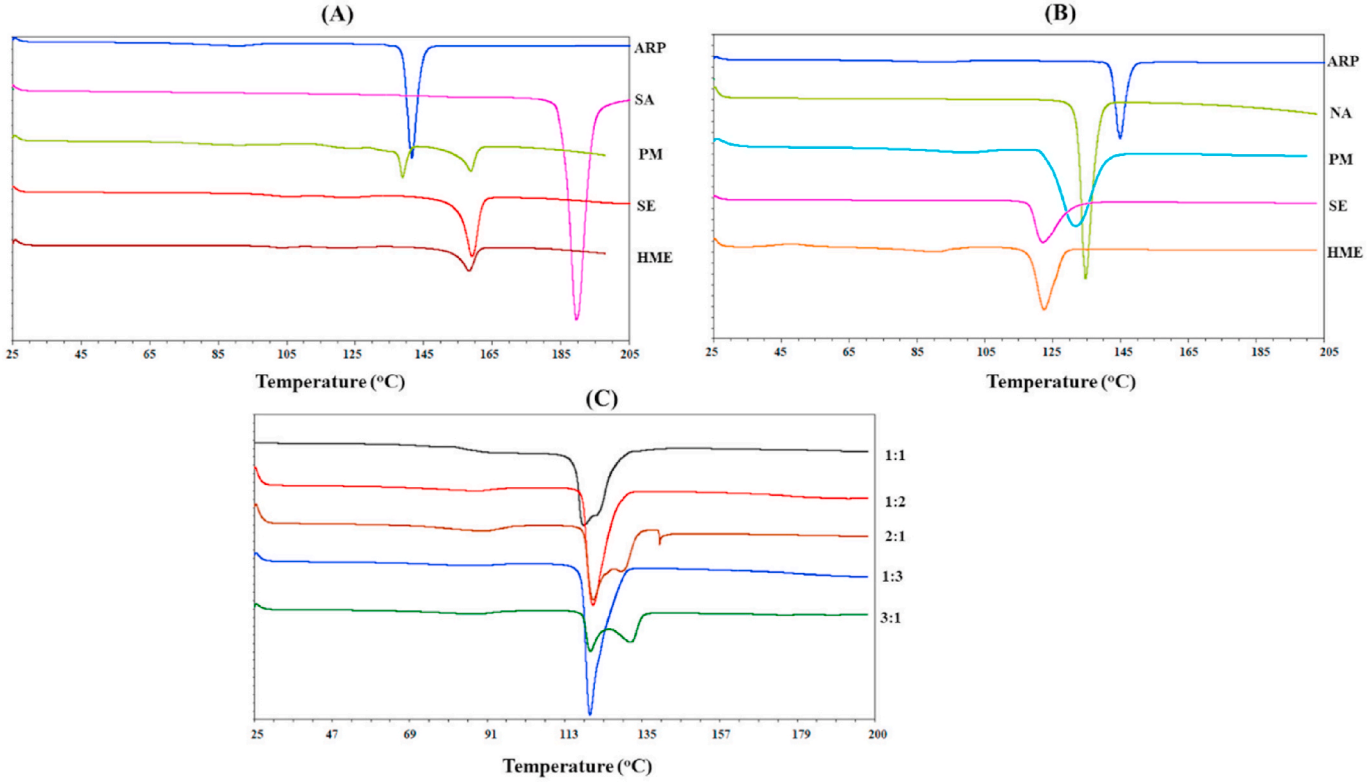

Fig. 3. DSC thermograms of A) the ARP-SA and B) ARP-NA systems produced via HME and C) an overlay plot of ARP-NA binary mixtures at 1:1, 1:2, 1:3, 2:1, and 3:1 ratio.

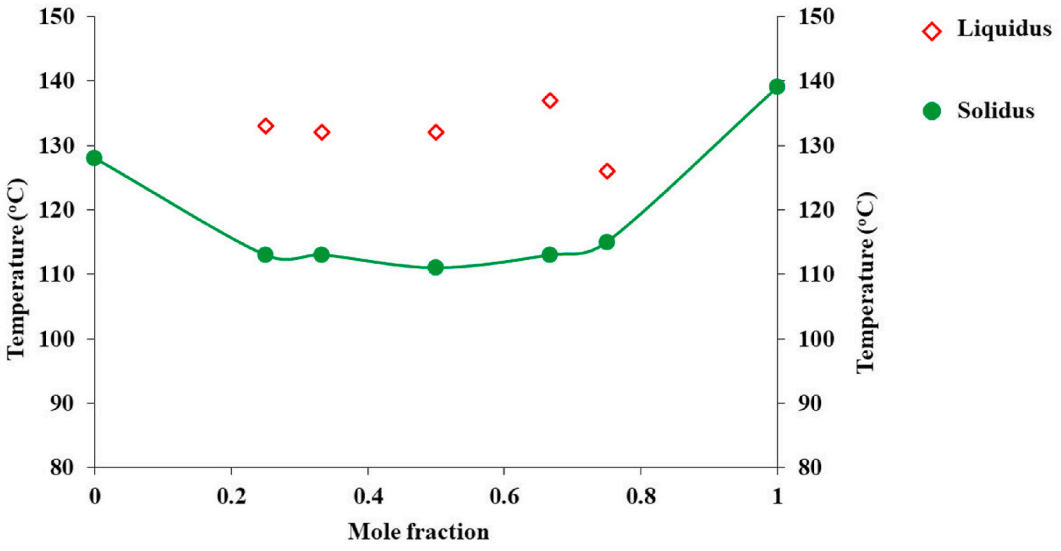

Fig. 4. Binary phase diagram of ARP-NA physical mixture samples.

systems should be studied in detail using techniques such as FTIR.

3.4. HSM

Physical transformation of the solid phase to a liquid phase in the ARP-SA and ARP-NA formulations was observed using HSM. The endothermic process of fusion and absorption of the latent heat of melting are the basic principles involved in HSM analysis [34]. Fig. 5A–B presents the melting behavior of the HME-produced ARP-SA and ARP-NA formulations.

In the ARP-SA system, melting behavior was observed for the crystalline material at 158 °C, indicating the salt/cocrystal formation temperature. In the case of the ARP-NA system, the physical transformation of the crystalline material from solid to liquid was observed at approximately 120 °C. These observed melting temperatures are attributed to the melting of newly formed solid states. No signs of thermal events or changes in melting behavior were observed until melting temperatures of 158 and 120 °C for ARP-SA and ARP-NA, respectively (Fig. 5). Thus, the complete melting at a single temperature is indicative of a single crystalline/eutectic entity without residual starting parent components and complete conversion of the individual components (drug and coformer) into a new solid material.

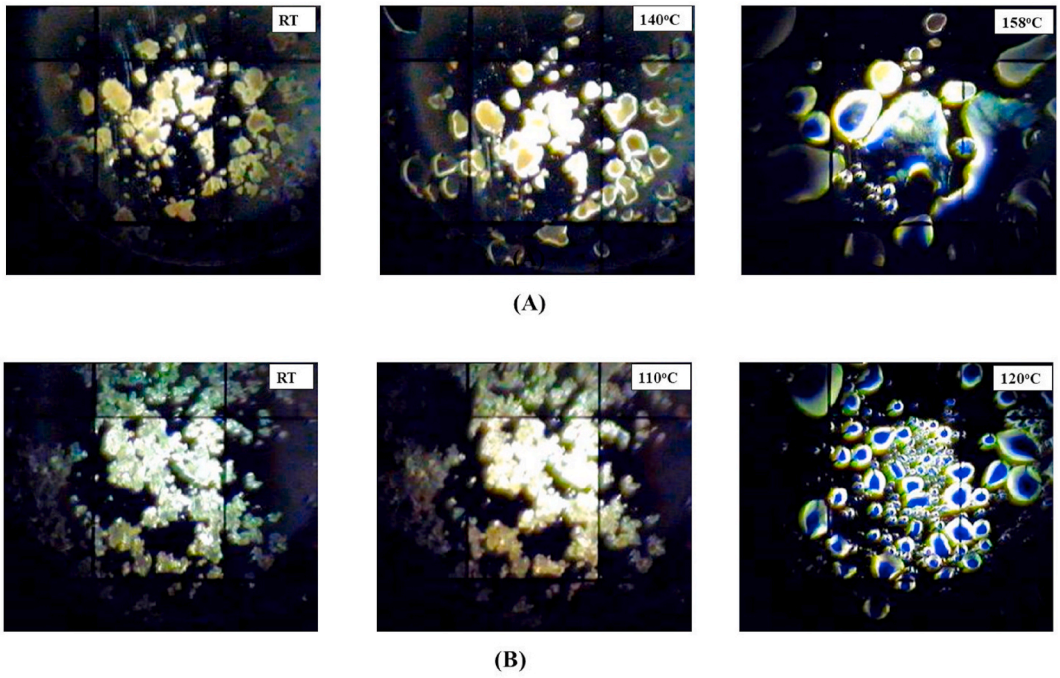

Fig. 5. HSM images of HME-produced A) ARP-SA and B) ARP-NA formulations.

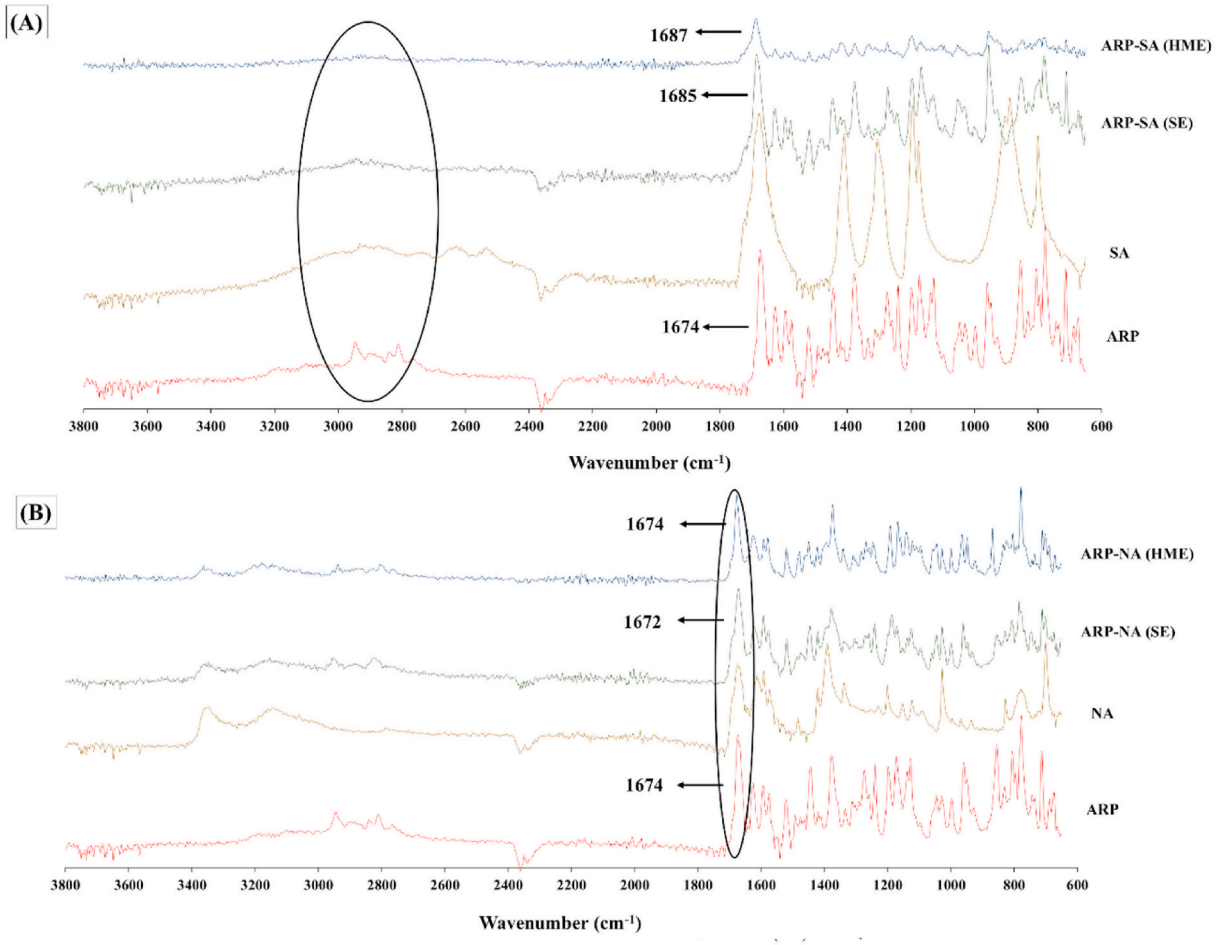

Fig. 6. FTIR spectra of the A) ARP-NA and B) ARP-SA multicomponent systems.

3.5. FTIR

The FTIR spectra of pure ARP, SA, NA and their HME formulations are presented in Fig. 6. FTIR spectroscopy can be used to predict the formation of salts, cocrystals and eutectics because any changes in the position of functional groups such as C═O and the intermolecular interactions between the drug and coformer can be examined using FTIR spectroscopy. In the FTIR spectrum of ARP-SA, the C═O stretching band of ARP at 1674 cm^{-1} is shifted to 1687 cm^{-1}, and this hypsochromic shift could be due to the weak hydrogen bonding (C–H- –O) between C═O of ARP and –CH of SA [35]. A new peak appeared at 1579 cm^{-1} and 1423 cm^{-1}, attributed to antisymmetric and symmetric stretching vibrations of carboxylate anions, suggesting the formation of salt [36,37].

The characteristic ARP bands at 2946 cm^{-1} and 2811 cm^{-1} disappeared, suggesting that the tertiary amine group ($N–CH_2$) was no longer in its primary state. This disappearance of the N–CH2 vibration bands at 2946 cm^{-1} and 2811 cm^{-1} indicated proton transfer between the N–CH2 (basic) of ARP and carboxylic groups (acidic) of SA. These observations suggest the formation of salt via proton transfer from the carboxylic groups of SA to the nitrogen atom in the tertiary amine group of ARP, as confirmed by the disappearance of N–CH2 stretching bands [38].

Brittain et al. [39] reported that the FTIR spectra of salts of benzoic acid revealed the absence of a carbonyl stretching band at 1629 cm^{-1} and the appearance of a carboxylate anion band at 1518 cm^{-1}, confirming the formation of a benzylammonium benzoate salt. Generally, salt formation can occur via ionic interactions with possible proton transfer. Thus, the FTIR spectrum of ARP-SA confirmed the occurrence of proton transfer between acidic and basic components. The FTIR spectrum of HME-processed ARP-NA shows IR bands with no major shift in -NH2 stretching bands from those in NA and displays no new bands or disappearance of the existing bands of ARP and NA. The carbonyl (C═O) bands in the resultant ARP-NA formulation display no major change in band positions and match well with the bands for the parent starting components, indicating weak adhesive interactions between ARP and NA [8]. Furthermore, the lack of a change/shift in the frequency of the C═O band suggested the absence of intermolecular interactions between ARP and NA. These observations suggest that the microstructure of the eutectics matches the lattice structure of the individual parent components, as evidenced by the absence of a new crystalline solid phase [9]. These observations are in accordance with the previous literature. Afrooz et al. [40], investigated the salts of aripiprazole with maleic acid, citric acid and tartaric acid by solubilization-crystallization methods. FTIR results showed disappearance, shift of some the bands, and appearance of new bands which were entirely different from the parent components. These findings indicated the formation of salts due to hydrogen bonding and ionic interaction between the drug and coformer. Araya-Sibaja et al. [41], prepared eutectics of lovastatin (LOV) with benzoic acid, salicylic acid and cinnamic acid. FTIR results confirmed that no major shifts in the FTIR band position of LOV compared to the individual components suggesting that there were no molecular interactions in the solid state, confirming the formation of a eutectic mixture.

The formation of salts or cocrystals can be distinguished by proton transfer or proton sharing between the drug and coformer. Salt formation involves acid-base reactions and proton transfer between a drug and a coformer. However, cocrystal formation pertains to bond motifs such as hydrogen bonding (proton sharing) between the functional groups of the drug and coformer rather than proton transfer [42]. Overall, the FTIR results confirmed the disappearance and appearance of new peaks in the ARP-SA system, indicating proton transfer and the formation of salts. The lack of a shift in C═O stretching band of ARP in the ARP-NA system indicated the formation of a eutectic.

3.6. PXRD analysis

The PXRD patterns of ARP and the coformers (SA and NA) were compared with those of their respective salts or eutectics to identify any structural differences. The diffractograms of pure ARP and the coformers indicated their crystalline nature (Fig. 7). The diffractogram of ARP showed major reflection peaks at 2θ values of 16.46°, 19.36°, 20.22°, 21.82°, and 24.68 [18]. Pure SA and NA showed characteristic peaks at 16.16°, 18.96°, 20.04°, 26.1°, 31.46°, 38.05°, and 38.50° and at 14.86°, 22.26°, 23.38°, 25.84°, and 27.32°, respectively [33,43,44]. The diffractogram of ARP-SA showed unique reflection peaks at 15.78°, 17.24°, and 17.84°, and these unique characteristic peaks in the salt were absent in the individual parent components. The diffraction peaks of SA at 26.1°, 31.46°, 38.05°, 38.50° disappeared in the ARP-SA salts, suggesting the formation of a new crystalline solid phase. The diffractogram of ARP-NA predominantly exhibited a combination of the peaks of both ARP and NA with slight changes in peak positions, and no new peaks or disappearance of characteristic peaks were observed in the diffractogram. These observations indicated the absence of a new crystalline solid phase and confirmed eutectic formation between ARP and NA [8]. The decrease in intensity of the reflection peaks in the HME-processed samples might be due to the smaller percentage of an amorphous mixture in the obtained samples. This finding is in accordance with the DSC results, where the intensities of the thermograms of the HME-processed samples are lower than those of the pure components, indicating a small fraction of amorphous material in the obtained extrudate samples.

Naqvi et al. [45] prepared atorvastatin calcium (AC) cocrystals using citric acid (CA) as a coformer. They observed distinct new peaks in the cocrystals with a decrease in their intensity compared to diffractograms of pure AC and CA, indicating the slightly amorphous nature of the formulation.

3.7. SEM analysis

The morphology of ARP, the coformers and the obtained product samples are presented in Fig. 8. ARP showed broken irregular plate-like crystals. The coformer SA was in the form of disk-shaped crystals with rough surfaces, while NA showed pebble-shaped crystals with tight packing.

The morphology of the HME-processed ARP-NA formulation was clumped and block-shaped, and crystals were fused with each other as spherical agglomerates with smooth surfaces, which differed from the bulk materials. The HME-treated ARP-SA showed flaky, irregularly shaped crystals with a smaller particle size distribution than observed for the pure components. These changes in the shape of the HME-produced samples can be explained by interactions between the drug and coformer molecules, which result in modification of the morphology of ARP. Furthermore, the intense mixing within the barrel of the extruder also contributed to the morphological (size and shape) changes of the obtained samples. The morphological characteristics have a great influence on the flowability, dissolution behavior and tableting behavior of APIs [46]. Previous reports in the literature revealed substantial enhancement of the mechanical properties of APIs through the formation of cocrystals/salts [47].

3.8. Solubility and in vitro dissolution

The solubility of ARP, eutectics and salts were found to be 2.8 ± 0.4, 18.3 ± 3.7 and 768 ± 68.3 μg/mL, respectively. In vitro dissolution studies were carried out to determine the performance of the produced salts and eutectics compared to bulk ARP. The dissolution rate of 2.4 μg/mL was observed for bulk ARP after 2 h (Fig. 9). In contrast, HME-produced salts showed a significant improvement in dissolution rate, with a value of 14.5 μg/mL at 2 h. The increase in dissolution rate was 6-fold in the salts compared to that of ARP. This improvement in the

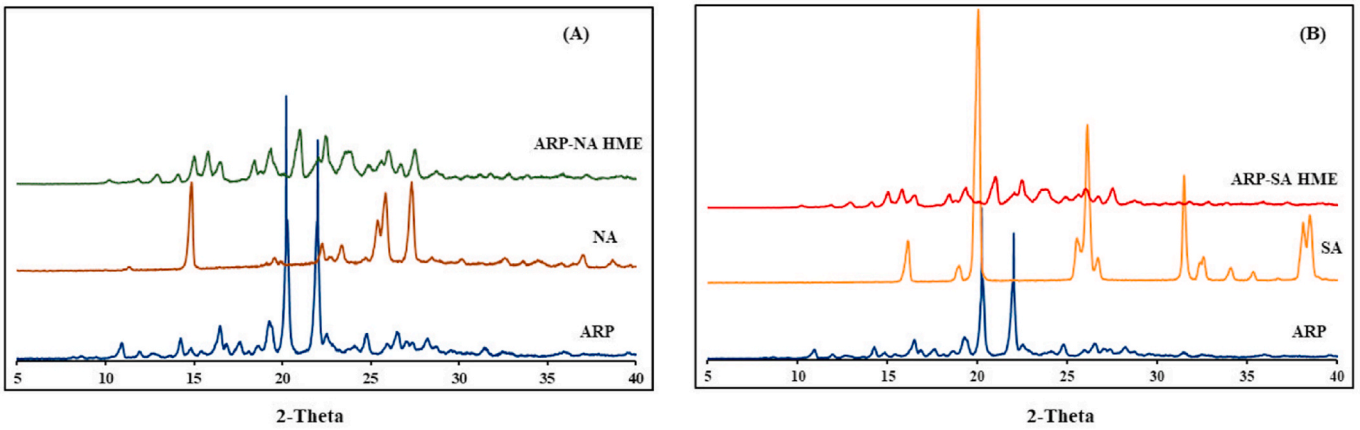

Fig. 7. PXRD diffractograms of the A) ARP-NA and B) ARP-SA multicomponent systems.

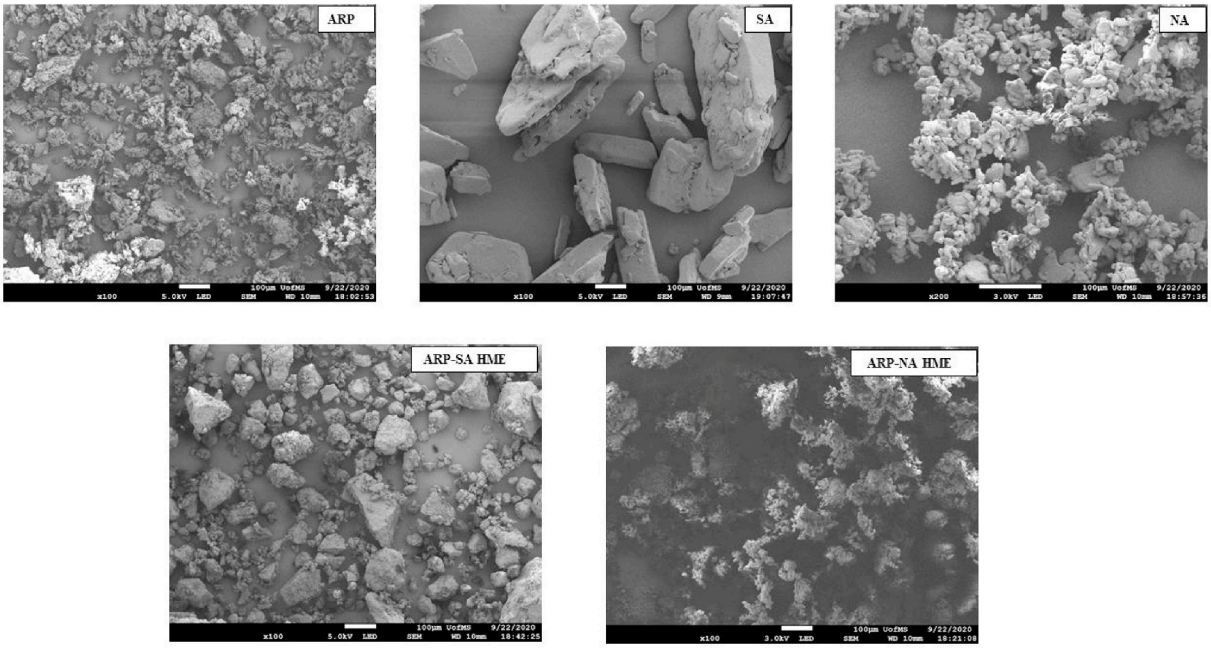

Fig. 8. SEM images of the drug, coformers and HME-processed multicomponent systems.

dissolution rate of ARP-SA was attributed to the interaction between ARP and SA and the formation of salt in situ during the extrusion process. Owing to the acidic characteristics of SA, the microenvironmental pH of the dissolution medium was decreased by SA, which could have resulted in an enhanced dissolution rate of ARP.

In the case of ionizable drugs (such as ARP), the microenvironment pH may differ from bulk pH, whereas for nonionizable drugs, the microenvironment pH and bulk pH may not vary. However, the presence of ionizable coformers in the cocrystals of nonionizable drugs may also lead to changes in microenvironment pH [48]. The magnitude of the increase in the dissolution rate of the salts can also be explained by their influence on the wettability, and thereby the diffusion layer thickness, of ARP in the dissolution medium [49].

The dissolution rate of ARP from the eutectics was observed to be 4.1 μg/mL, which is 1.7-fold higher than that of bulk ARP. This slight increase in dissolution rate might be due to the difference in particle size between ARP and the HME-processed eutectics. The improved hydrophilicity of ARP in the eutectic system due to the presence of hydrophilic NA could also be responsible for the enhanced dissolution rate of ARP in the ARP-NA eutectic. Good and Rodriguez-Hornedo [50] proposed that a coformer solubility of at least 10 times the pure drug solubility is needed for multicomponent solid systems to exhibit a better solubility and dissolution rate profile than the pure drug.

Since the aqueous solubility values of SA and NA are greater than those of ARP (SA: 71 mg/mL and NA: > 100 mg/mL), the presence of coformers may appear to improve the dissolution profile of ARP. The coformers SA and NA are freely soluble in water, and their aqueous solubility is > 100-fold higher than that of ARP, which might be one of the reasons for the improved dissolution rate of ARP. The improved dissolution rate of ARP in the obtained salts and eutectics can be explained by the microenvironmental pH, the aqueous solubility of the coformers and the interactions between the drug and coformers [4]. Thus, these parameters are key factors for the enhanced dissolution rate of ARP in the salt and eutectic systems.

3.9. Measurement of microenvironment pH

To investigate the influence of the coformers on the dissolution profiles of the ARP multicomponent crystalline solid systems, the microenvironmental solution pH was measured after suspending the

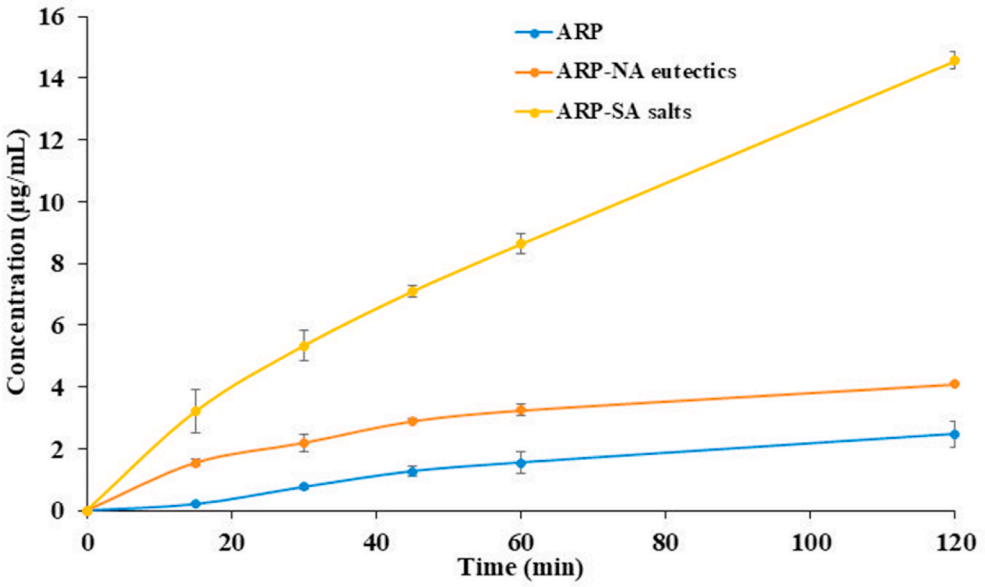

Fig. 9. Dissolution profiles of ARP, ARP-SA and ARP-NA formulations.

samples in DI water for 24 h. The pH formed at the dissolving surface containing saturated solid particles represents the microenvironment pH [48]. For drugs with pH-dependent solubility, it was reported that the pH of the dissolution medium greatly influences the dissolution rate, suggesting that microenvironmental pH is one factor that can affect the dissolution behavior and in turn the bioavailability of poorly soluble drugs [28]. The coformers (SA and NA) and pure ARP had microenvironmental pH values of 2.06, 7.45 and 7.25, respectively.

The ARP-SA salt system had a microenvironmental pH of 3.62, much lower than that of pure ARP. This change in microenvironmental pH was due to the presence of the coformer (SA), which decreased the solution pH owing to its carboxylic acid groups and increased the dissolution of ARP. The decrease in the microenvironmental pH of the ARP-NA system was less prominent and, and the value was comparable to the solution pH of ARP, which was originally 7.25, while the eutectic system showed a microenvironmental pH of 7.28.

These observations indicate that the presence of an acid coformer in the ARP-SA salt system resulted in more acidity of the ARP solution. For the salts, the microenvironmental pH results correlate well with the increased dissolution rate of ARP. Since the microenvironmental pH of the eutectics is comparable to the solution pH of ARP, the correlation of dissolution rate with microenvironment pH is less prominent. Maddileti et al. [51] developed cocrystals of febuxostat with acidic (p-amino benzoic acid) and basic coformers (acetamide, nicotinamide, and urea). The cocrystals produced with basic coformers exhibited a greater dissolution rate than the cocrystals made of acidic coformers, demonstrating the effects of acidic and basic coformers on the dissolution rate of poorly soluble drugs.

4. Conclusion

HME as a continuous manufacturing technique was explored for the development of salts and eutectics of ARP with selected coformers (SA and NA). The single melting temperature in the DSC thermograms of the HME-processed formulations was attributed to the molecular arrangement with the possible formation of a new solid crystalline material. The close melting temperatures of the parent components (ARP and NA) resulted in a single endothermic peak in the PM samples; for such systems, thermal analysis (DSC) may not differentiate between eutectics and cocrystals. The shifts, appearance or disappearance of peaks in the FTIR spectra and PXRD diffractograms revealed the formation of a new crystalline solid material in the ARP-SA system. In the case of ARP-NA, there were no shifts in the C═O stretching band in the FTIR spectra, suggesting the absence of intermolecular interactions and thus no formation of a new crystalline material. The HME-processed multicomponent crystalline solid forms exhibited an increased dissolution rate compared with that of the pure drug. It is worth mentioning that the ARP-SA system displayed a higher dissolution rate than ARP-NA due to the significant change in microenvironment pH compared with that of the pure drug. Furthermore, to identify and confirm the formation of new crystalline material, additional characterization tools such as solid-state NMR and single-crystal XRD studies in particular can help differentiate salts and cocrystals.

Funding

This project was partially supported by Grant Number P30GM122733-01A1 funded by the National Institute of General Medical Sciences (NIGMS), a component of the National Institutes of Health (NIH) as one of its Centers of Biomedical Research Excellence (COBRE).

Author contributions

Arun Butreddy, Suresh Bandari, and Michael Repka designed the study. Arun Butreddy, Mashan Almutairi, Neeraja Komanduri, performed the experiments and analyzed the data. The performance and analysis of XRD data by Feng Zhang. Arun Butreddy wrote the manuscript, review and editing Suresh Bandari, supervision and manuscript editing was by Michael A. Repka.

Declaration of competing interest

The authors declare no conflicts of interest.

Acknowledgments

The scanning electron microscopy images presented in this work were generated using the instruments and services at the Microscopy and Imaging Center, The University of Mississippi. This facility is supported in part by grant 1726880, National Science Foundation.

References

[1] N. Schultheiss, A. Newman, Pharmaceutical cocrystals and their physicochemical properties, Cryst. Growth Des. 9 (2009) 2950–2967, https://doi.org/10.1021/cg900129f.

[2] S. Cherukuvada, T.N. Guru Row, Comprehending the formation of eutectics and cocrystals in terms of design and their structural interrelationships, Cryst. Growth Des. 14 (2014) 4187–4198, https://doi.org/10.1021/cg500790q.

[3] A. Shevchenko, L.M. Bimbo, I. Miroshnyk, J. Haarala, K. Jelínková, K. Syrjänen, B. van Veen, J. Kiesvaara, H.A. Santos, J. Yliruusi, A new cocrystal and salts of itraconazole: comparison of solid-state properties, stability and dissolution behavior, Int. J. Pharm. 436 (2012) 403–409, https://doi.org/10.1016/j.ijpharm.2012.06.045.

[4] M. Karimi-Jafari, L. Padrela, G.M. Walker, D.M. Croker, Creating cocrystals: a review of pharmaceutical cocrystal preparation routes and applications, Cryst. Growth Des. 18 (2018) 6370–6387, https://doi.org/10.1021/acs.cgd.8b00933.

[5] R. Shaikh, R. Singh, G.M. Walker, D.M. Croker, Pharmaceutical cocrystal drug products: an outlook on product development, Trends Pharmacol. Sci. 39 (2018) 1033–1048, https://doi.org/10.1016/j.tips.2018.10.006.

[6] Z. Rahman, R. Samy, V.A. Sayeed, M.A. Khan, Physicochemical and mechanical properties of carbamazepine cocrystals with saccharin, Pharmaceut. Dev. Technol. 17 (2012) 457–465, https://doi.org/10.3109/10837450.2010.546412.

[7] S. Tsutsumi, M. Iida, N. Tada, T. Kojima, Y. Ikeda, T. Moriwaki, K. Higashi, K. Moribe, K. Yamamoto, Characterization and evaluation of miconazole salts and cocrystals for improved physicochemical properties, Int. J. Pharm. 421 (2011) 230–236, https://doi.org/10.1016/j.ijpharm.2011.09.034.

[8] S. Cherukuvada, A. Nangia, Eutectics as improved pharmaceutical materials: design, properties and characterization, Chem. Commun. 50 (2013) 906–923, https://doi.org/10.1039/C3CC47521B.

[9] C.B.M. Figueirêdo, D. Nadvorny, A.C.Q. de Medeiros Vieira, J.L. Soares Sobrinho, P.J. Rolim Neto, P.I. Lee, M.F. de La Roca Soares, Enhancement of dissolution rate through eutectic mixture and solid solution of posaconazole and benznidazole, Int. J. Pharm. 525 (2017) 32–42, https://doi.org/10.1016/j.ijpharm.2017.04.021.

[10] R. Kaur, R. Gautam, S. Cherukuvada, T.N. Guru Row, Do carboximide-carboxylic acid combinations form co-crystals? The role of hydroxyl substitution on the formation of co-crystals and eutectics, IUCrJ 2 (2015) 341–351, https://doi.org/10.1107/S2052252515002651.

[11] G.J. Fernandes, M. Rathnanand, V. Kulkarni, Mechanochemical synthesis of carvedilol cocrystals utilizing hot melt extrusion technology, J. Pharm. Innov. 14 (2019) 373–381, https://doi.org/10.1007/s12247-018-9360-y.

[12] S. Narala, D. Nyavanandi, P. Srinivasan, P. Mandati, S. Bandari, M.A. Repka, Pharmaceutical Co-crystals, Salts, and Co-amorphous Systems: a novel opportunity of hot-melt extrusion, J. Drug Deliv. Sci. Technol. (2020), 102209, https://doi.org/10.1016/j.jddst.2020.102209.

[13] M. Maniruzzaman, D.J. Morgan, A.P. Mendham, J. Pang, M.J. Snowden, D. Douroumis, Drug-polymer intermolecular interactions in hot-melt extruded solid dispersions, Int. J. Pharm. 443 (2013) 199–208, https://doi.org/10.1016/j.ijpharm.2012.11.048.

[14] M. Gajda, K.P. Nartowski, J. Pluta, B. Karolewicz, The role of the polymer matrix in solvent-free hot melt extrusion continuous process for mechanochemical synthesis of pharmaceutical cocrystal, Eur. J. Pharm. Biopharm. 131 (2018) 48–59, https://doi.org/10.1016/j.ejpb.2018.07.002.

[15] J.B. Nanubolu, K. Ravikumar, Correlating the melting point alteration with the supramolecular structure in aripiprazole drug cocrystals, CrystEngComm 18 (2016) 1024–1038, https://doi.org/10.1039/C5CE02400E.

[16] M.-Y. Cho, P. Kim, G.-Y. Kim, J.-Y. Lee, K.-H. Song, M.-J. Lee, W. Yoon, H. Yun, G. J. Choi, Preparation and characterization of aripiprazole cocrystals with coformers of multihydroxybenzene compounds, Cryst. Growth Des. 17 (2017) 6641–6652, https://doi.org/10.1021/acs.cgd.7b01281.

[17] A.F. Casares, W.M. Nap, G.T. Figás, P. Huizenga, R. Groot, M. Hoffmann, An evaluation of salt screening methodologies, J. Pharm. Pharmacol. 67 (2015) 812–822, https://doi.org/10.1111/jphp.12377.

[18] A. Butreddy, S. Sarabu, S. Bandari, N. Dumpa, F. Zhang, M.A. Repka, Polymer-assisted aripiprazole–adipic acid cocrystals produced by hot melt extrusion techniques, Cryst. Growth Des. 20 (2020) 4335–4345, https://doi.org/10.1021/acs.cgd.0c00020.

[19] C.C. Seaton, A. Parkin, Making benzamide cocrystals with benzoic acids: the influence of chemical structure, Cryst. Growth Des. 11 (2011) 1502–1511.

[20] S. Koranne, J.F. Krzyzaniak, S. Luthra, K.K. Arora, R. Suryanarayanan, Role of coformer and excipient properties on the solid-state stability of theophylline cocrystals, Cryst. Growth Des. 19 (2019) 868–875, https://doi.org/10.1021/acs.cgd.8b01430.

[21] K.L. Cavanagh, C. Maheshwari, N. Rodríguez-Hornedo, Understanding the differences between cocrystal and salt aqueous solubilities, J. Pharmaceut. Sci. 107 (2018) 113–120, https://doi.org/10.1016/j.xphs.2017.10.033.

[22] E. Lu, N. Rodríguez-Hornedo, R. Suryanarayanan, A rapid thermal method for cocrystal screening, CrystEngComm 10 (2008) 665–668, https://doi.org/10.1039/B801713C.

[23] I. Sathisaran, J.M. Skieneh, S. Rohani, S.V. Dalvi, Curcumin eutectics with enhanced dissolution rates: binary phase diagrams, characterization, and dissolution studies, J. Chem. Eng. Data 63 (2018) 3652–3671, https://doi.org/10.1021/acs.jced.7b01105.

[24] E.B. Ferreira, M.L. Lima, E.D. Zanotto, DSC method for determining the liquidus temperature of glass-forming systems, J. Am. Ceram. Soc. 93 (2010) 3757–3763.

[25] S.I.F. Badawy, M.A. Hussain, Microenvironmental pH modulation in solid dosage forms, J. Pharm. Sci. 96 (2007) 948–959, https://doi.org/10.1002/jps.20932.

[26] S. Li, T. Yu, Y. Tian, C.P. McCoy, D.S. Jones, G.P. Andrews, Mechanochemical synthesis of pharmaceutical cocrystal suspensions via hot melt extrusion: feasibility studies and physicochemical characterization, Mol. Pharmaceut. 13 (2016) 3054–3068, https://doi.org/10.1021/acs.molpharmaceut.6b00134.

[27] S. Korde, S. Pagire, H. Pan, C. Seaton, A. Kelly, Y. Chen, Q. Wang, P. Coates, A. Paradkar, Continuous manufacturing of cocrystals using solid state shear milling technology, Cryst. Growth Des. 18 (2018) 2297–2304, https://doi.org/10.1021/acs.cgd.7b01733.

[28] M. Jagia, R. Daptardar, K. Patel, A.K. Bansal, S. Patel, Role of structure, microenvironmental pH, and speciation to understand the formation and properties of febuxostat eutectics, Mol. Pharm. 16 (2019) 4610–4620, https://doi.org/10.1021/acs.molpharmaceut.9b00716.

[29] H. Yamashita, Y. Hirakura, M. Yuda, T. Teramura, K. Terada, Detection of cocrystal formation based on binary phase diagrams using thermal analysis, Pharm. Res. (N. Y.) 30 (2013) 70–80, https://doi.org/10.1007/s11095-012-0850-1.

[30] H. Yamashita, Y. Hirakura, M. Yuda, K. Terada, Coformer screening using thermal analysis based on binary phase diagrams, Pharmaceut. Res. 31 (2014) 1946–1957.

[31] H.-L. Lin, G.-C. Zhang, Y.-T. Huang, S.-Y. Lin, An investigation of indomethacin-nicotinamide cocrystal formation induced by thermal stress in the solid or liquid state, J. Pharm. Sci. 103 (2014) 2386–2395, https://doi.org/10.1002/jps.24056.

[32] A.N. Manin, A.P. Voronin, K.V. Drozd, N.G. Manin, A. Bauer-Brandl, G.L. Perlovich, Cocrystal screening of hydroxybenzamides with benzoic acid derivatives: a comparative study of thermal and solution-based methods, Eur. J. Pharmaceut. Sci. 65 (2014) 56–64, https://doi.org/10.1016/j.ejps.2014.09.003.

[33] C.A. Ober, R.B. Gupta, formation of itraconazole–succinic acid cocrystals by gas antisolvent cocrystallization, AAPS PharmSciTech 13 (2012) 1396–1406, https://doi.org/10.1208/s12249-012-9866-4.

[34] K. Chadha, M. Karan, R. Chadha, Y. Bhalla, K. Vasisht, Is failure of cocrystallization actually a failure? eutectic formation in cocrystal screening of hesperetin, J. Pharm. Sci. 106 (2017) 2026–2036, https://doi.org/10.1016/j.xphs.2017.04.038.

[35] L. Rajput, Stable crystalline salts of haloperidol: a highly water-soluble mesylate salt, Cryst. Growth Des. 14 (2014) 5196–5205, https://doi.org/10.1021/cg500982u.

[36] K.A. Solomon, O. Blacque, R. Venkatnarayan, Molecular salts of 2,6-dihydroxybenzoic acid (2,6-DHB) with N-heterocycles: crystal structures, spectral properties and Hirshfeld surface analysis, J. Mol. Struct. 1134 (2017) 190–198, https://doi.org/10.1016/j.molstruc.2016.12.055.

[37] L.F. Diniz, P.S. Carvalho, S.A.C. Pena, J.E. Gonçalves, M.A.C. Souza, J.D. de Souza Filho, L.F.O. Bomfim Filho, C.H.J. Franco, R. Diniz, C. Fernandes, Enhancing the solubility and permeability of the diuretic drug furosemide via multicomponent crystal forms, Int. J. Pharm. 587 (2020), 119694, https://doi.org/10.1016/j.ijpharm.2020.119694.

[38] H.L. Lee, J.M. Vasoya, M. de L. Cirqueira, K.L. Yeh, T. Lee, A.T.M. Serajuddin, Continuous preparation of 1:1 haloperidol–maleic acid salt by a novel solvent-free method using a twin screw melt extruder, Mol. Pharmaceut. 14 (2017) 1278–1291, https://doi.org/10.1021/acs.molpharmaceut.7b00003.

[39] H.G. Brittain, Vibrational spectroscopic studies of cocrystals and salts. 1. The Benzamide−Benzoic acid system, Cryst. Growth Des. 9 (2009) 2492–2499, https://doi.org/10.1021/cg801397t.

[40] H. Afrooz, E.M. Mohamed, S.F. Barakh Ali, S. Dharani, M.T.H. Nutan, M.A. Khan, Z. Rahman, Salt engineering of aripiprazole with polycarboxylic acids to improve physicochemical properties, AAPS PharmSciTech 22 (2021) 31, https://doi.org/10.1208/s12249-020-01875-x.

[41] A.M. Araya-Sibaja, J.R. Vega-Baudrit, T. Guillén-Girón, M. Navarro-Hoyos, S. L. Cuffini, Drug solubility enhancement through the preparation of multicomponent organic materials: eutectics of lovastatin with carboxylic acids, Pharmaceutics 11 (2019) 112, https://doi.org/10.3390/pharmaceutics11030112.

[42] Early Drug Development: Bringing a Preclinical Candidate to the Clinic, 2 Volume Set | Wiley, (n.d.). https://www.wiley.com/en-by/Early+Drug+Development%3A+Bringing+a+Preclinical+Candidate+to+the+Clinic%2C+2+Volume+Set-p-9783527801756 (accessed October 2, 2020).

[43] G. Bruni, F. Monteforte, L. Maggi, V. Friuli, C. Ferrara, P. Mustarelli, A. Girella, V. Berbenni, D. Capsoni, C. Milanese, A. Marini, Probenecid and benzamide: cocrystal prepared by a green method and its physico-chemical and pharmaceutical characterization, J. Therm. Anal. Calorim. 140 (2020) 1859–1869, https://doi.org/10.1007/s10973-019-09197-2.

[44] Y. Yuliandra, E. Zaini, S. Syofyan, W. Pratiwi, L.N. Putri, Y.S. Pratiwi, H. Arifin, Cocrystal of ibuprofen–nicotinamide: solid-state characterization and in vivo analgesic activity evaluation, Sci. Pharm. 86 (2018) 23, https://doi.org/10.3390/scipharm86020023.

[45] A. Naqvi, M. Ahmad, M.U. Minhas, K.U. Khan, F. Batool, A. Rizwan, Preparation and evaluation of pharmaceutical co-crystals for solubility enhancement of atorvastatin calcium, Polym. Bull. (2019) 1–21.

[46] P. Szabó-Révész, H. Göczö, K. Pintye-Hódi, P. Kása, I. Erös, M. Hasznos-Nezdei, B. Farkas, Development of spherical crystal agglomerates of an aspartic acid salt for direct tablet making, Powder Technol. 114 (2001) 118–124, https://doi.org/10.1016/S0032-5910(00)00272-2.

[47] R.S. Dhumal, A.L. Kelly, P. York, P.D. Coates, A. Paradkar, Cocrystalization and simultaneous agglomeration using hot melt extrusion, Pharm. Res. (N. Y.) 27 (2010) 2725–2733, https://doi.org/10.1007/s11095-010-0273-9.

[48] D.P. Kale, S.S. Zode, A.K. Bansal, Challenges in translational development of pharmaceutical cocrystals, J. Pharm. Sci. 106 (2017) 457–470, https://doi.org/10.1016/j.xphs.2016.10.021.

[49] D.P. Elder, R. Holm, H.L. de Diego, Use of pharmaceutical salts and cocrystals to address the issue of poor solubility, Int. J. Pharm. 453 (2013) 88–100, https://doi.org/10.1016/j.ijpharm.2012.11.028.

[50] D.J. Good, N. Rodriguez-Hornedo, Solubility advantage of pharmaceutical cocrystals, Cryst. Growth Des. 9 (2009) 2252–2264.

[51] D. Maddileti, S.K. Jayabun, A. Nangia, Soluble cocrystals of the xanthine oxidase inhibitor febuxostat, Cryst. Growth Des. 13 (2013) 3188–3196.